Journal of Structural Geology, Vol. 8, No. 2, pp. 101 to 109, 1986
Printed in Great Britain

0191-8141/86 $03.00 + 0.00

A determination of the bulk rotational deformation resulting from displacements in discrete shear zones in the Hercynian Fold Belt of South Ireland

DENIS A. COLLINS

Geology Department, University College, Cork, Ireland

and

DECLAN G. DE PAOR

Department of Earth & Planetary Sciences, Johns Hopkins University, Baltimore, MD 21218, U.S.A.

(*Received* 10 *August* 1984; *accepted in revised form* 10 *May* 1985)

Abstract—In the Hercynian Fold Belt of South Ireland, near the town of Ardmore, County Waterford, units of openly folded Upper Palaeozoic sandstone and siltstone are traversed by closely spaced arrays of en échelon quartz veins. These arrays mark the sites of shear zones which are bounded by weakly deformed wall rocks. We used the attitude of cleavage and the sigmoidal shapes of veins to calculate the cumulative shear strain across each zone, and then determined the bulk deformation suffered by the outcrop by tensor analysis, with the aid of an off-axis Mohr circle construction. We conclude that, as a consequence of vein formation, the rocks at this outcrop suffered significant bulk deformation with an 8–14° clockwise rotation.

INTRODUCTION

THE QUANTITATIVE analysis of deformation in rocks is generally based on one of two different approaches. First, using deformed objects such as fossils or conglomerate pebbles, the irrotational component of deformation may be determined over a continuous and intact domain of rock (e.g. Ramsay & Huber 1983). Second, the discrete movement on faults may be determined from their geometric effects on lithology, and the displacements reversed by techniques such as section-balancing (e.g. Hossack 1979). The deformation in shear zones is an intermediate case; such zones are discrete structures in the rock mass, yet within each zone, the strain may be continuous and quantifiable.

In this paper, we attempt to quantify the contribution of shear zones to the overall state of deformation in a bedding plane. We assume that each zone has suffered heterogeneous simple shear and that bedding is in the plane of monoclinic symmetry of the shear deformation.

The geometry and mechanics of en échelon veins have been studied previously by Roering (1968), Lajtai (1969) and Hancock (1972). Deformation-induced microstructural features within vein arrays have been analysed by Ramsay & Graham (1970), Beach (1975) and Knipe & White (1979). Ramsay (1980) has discussed the formation of 'extension fissures' by a crack–seal mechanism. Beach (1975) described the two-dimensional features of en échelon vein arrays in the Hercynian belt of South Wales. They were also the subject of an analysis on the mesoscopic and microscopic scales by Knipe & White (1979).

GEOLOGICAL SETTING

Detailed (25 inch to 1 mile scale) geological mapping was done in the Ardmore area of southwest County Waterford (Fig. 1). The area is dominated by a large E-trending syncline known as the Ardmore Syncline. It is cored by Waulsortian 'reef' limestone while on the southern limb a well-exposed coastal section shows a conformable sequence of alluvial Old Red Sandstone, represented here by the Kiltorcan Formation, overlain by Lower Carboniferous clastics of the Kinsale Group (see Collins 1985). The base of the Kinsale Group is marked by a 6 m thick dark grey mudstone unit, the Castle Slate Formation. The base of this formation may be equated with the Devonian Carboniferous boundary.

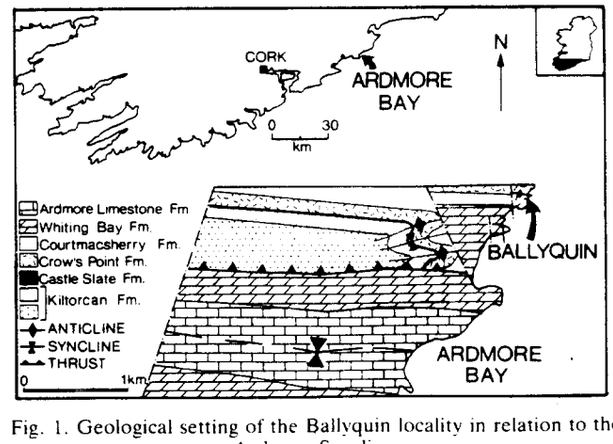

Fig. 1. Geological setting of the Ballyquin locality in relation to the Ardmore Syncline.

Overlying the Castle Slate Formation is approximately 28 m of massive grey quartzitic sandstones and a significant amount of quartz pebble conglomerate interbedded with pebbly sandstones. Near its base, this unit, the Crows Point Formation, contains thin sandstone beds alternating with thin flaser-bedded units.

The poorly exposed north limb of the Ardmore Syncline is truncated by a strike-parallel back thrust (Cooper *et al.* 1984, Collins 1985). This separates outcrops of calcareous Whiting Bay Formation and Old Red Sandstone, the latter defining an anticlinal ridge to the north (Fig. 1).

North of the Ardmore Syncline, at Ballyquin (grid reference X205799), a large N-trending wrench fault causes the upper Formation of the Kinsale Group, the Crows Point Formation, to abut against both the stratigraphically higher beds of the calcareous Whiting Bay Formation and the underlying Courtmacsherry Formation. The Crows Point Formation forms the host rock for well-developed conjugate sets of vein arrays. The Ballyquin locality is on the crest of an open anticline and bedding is beautifully exposed at low tide as wave polished surfaces. Although there are large-scale trough+cross-stratified units, the beds are mainly parallel sided with bed thickness ranging from 15 to 50 cm. Good joint sets have developed, forming a conjugate system of subvertical joints symmetric about strike. The competence of the lithologies enhances the development of good laterally traceable fractures and shear zones. Dawson-Grove (1955) first described the minor structures of the area in detail. He was one of the first structural geologists to draw attention to the relationship between en échelon vein arrays and zones of simple shear, although he did not use a modern nomenclature.

NATURE OF THE VEIN ARRAYS

The vein arrays occur as narrow, subparallel-walled conjugate sets within the sandstones at Ballyquin (Fig. 2). They vary in width from 20 to 100 mm at the centres of the zones. The zones may be classified as brittle–ductile shear zones (Ramsay 1980). They contain veins infilled with fibrous quartz and some chlorite. As a consequence of variations in the amount of shear displacement in the zones from centre to edge, the veins are sigmoidal in shape.

The tails of the extension fissures should theoretically be oriented at 45° to the shear zone boundaries (e.g. Hancock 1972). It was found, however, that this angle varied from 37 to 42° in the profile section of some of the larger, more sigmoidal fissures, implying a component of tension perpendicular to the zone (see Ramsay & Huber 1983). Small non-sigmoidal veins are seen making angles of approximately 45° to the zone boundaries. Some of these are bifurcating tails to larger extension fissures. Reactivation or prolonged continuous development of the shear zones has resulted in the superposition of numerous vein sets in some zones (Fig. 3).

Spaced cleavage planes varying in strike from 050 to 095° are developed in many of the shear zones. Their darkened appearance is highly suggestive of a pressure solution mechanism of formation and this is confirmed by thin section examination. Elongate growth fibres of quartz are found in the veins. The quartz crystals within the fibres are optically continuous across the veins. In general, the quartz grains in the host rock (which at Ballyquin may be classified as a quartz arenite) are up to 0.6 mm in diameter whereas in the veins they increase to more than 1.3 mm along their long axis. The elongate quartz grains contain a high concentration of inclusions (Fig. 4). An increase in the density of inclusions is evident towards the centres of some grains. Locally, the inclusions form linear trails oriented subperpendicular to the fibre direction.

Some sub-grains and also areas of incipient recrystallization of larger quartz grains are seen within the veins. The elongate grains have low-angle boundaries between them, and many of the grain walls are marked by pressure shadows and a dentate type of morphology (Fig. 5). Many of the grains display undulose extinction, deformation lamellae and also the development of microshear planes. Separated fragments of grains may be matched across fractures in some cases. Therefore, both ductile and brittle deformational structures are found within the en échelon arrays.

The host rock consists of detrital quartz grains and a minor amount of microcline which displays cross-hatch twinning. Evidence of strain is seen within the host rock and also within many of the larger grains displaying undulose extinction. Some features may have been inherited but cataclastic textures are also evident. Some grains are coated with chlorite and pressure-solution effects are evident at grain boundaries.

From an analysis of thin sections, the crystals of the host rock seem to have grown as fibres in the direction of maximum extension across the shear zone during the process of dilation of the veins. The overgrowths were probably enhanced by the supply of pressure-solution material. The presence of linear strings of inclusions within the quartz grains is consistent with the description by Ramsay (1980) of veins formed elsewhere by the crack–seal mechanism.

WALL-ROCK DEFORMATION

The state of deformation in the plane of bedding at the Ballyquin outcrop was studied in an area free of shear zones. The bedding plane chosen was densely packed with quartz pebbles which were analysed using the Rf/ϕ technique (Ramsay 1967, Dunnet 1969) as modified by De Paor (1981). The axial ratios, Rf, and long-axis orientations, ϕ, of sixteen pebbles were measured relative to an arbitrary reference direction and were plotted on log-polar graph paper (Fig. 6). The median long-axis orientation was taken as an estimate of the principal stretch direction which was approximately horizontal in this case. The axial ratio of the left-stretch ellipse was

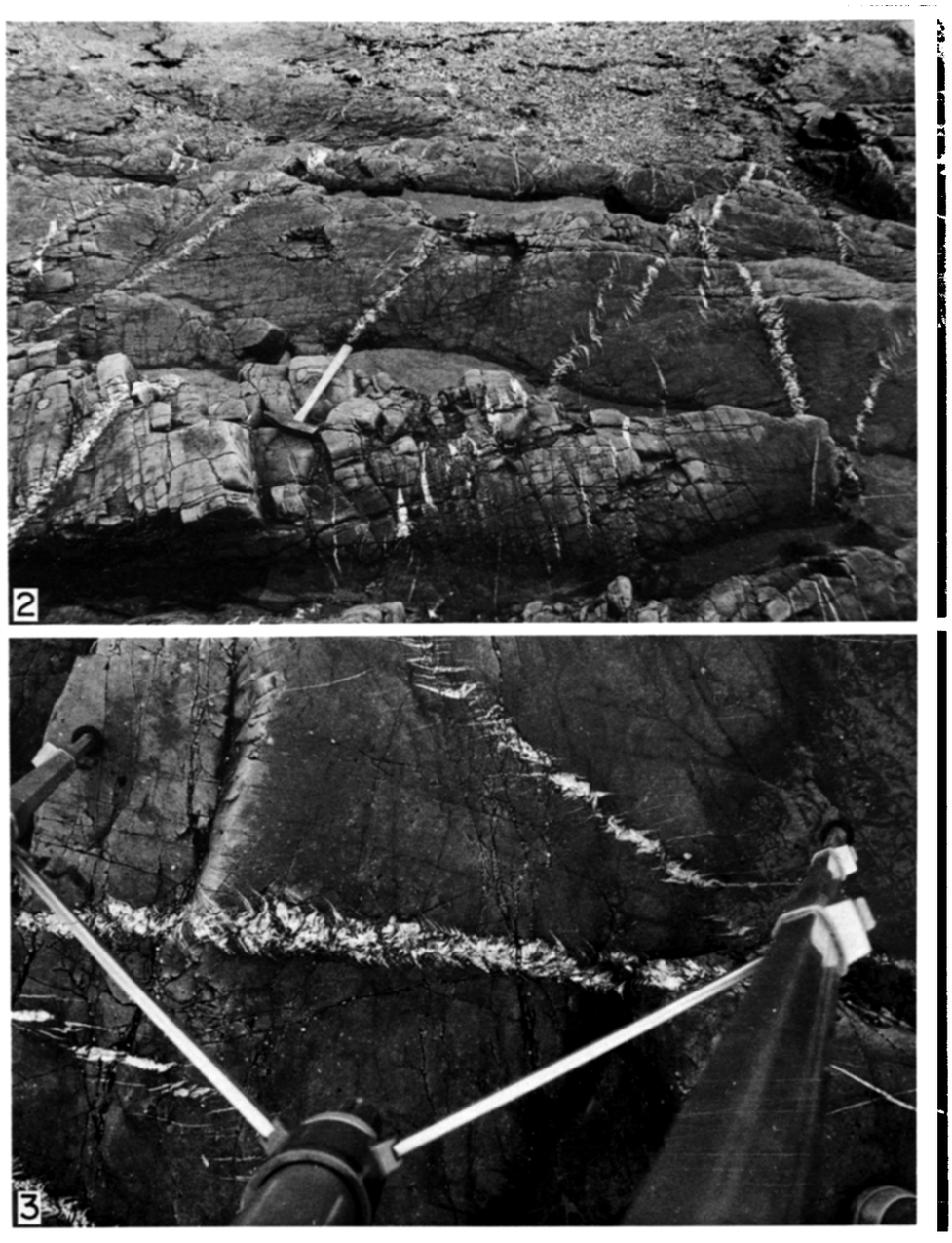

Fig. 2. Conjugate sets of en échelon vein arrays at Ballyquin Beach.

Fig. 3. Superposition of several vein sets in a single shear zone. Tripod legs are 1 metre apart.

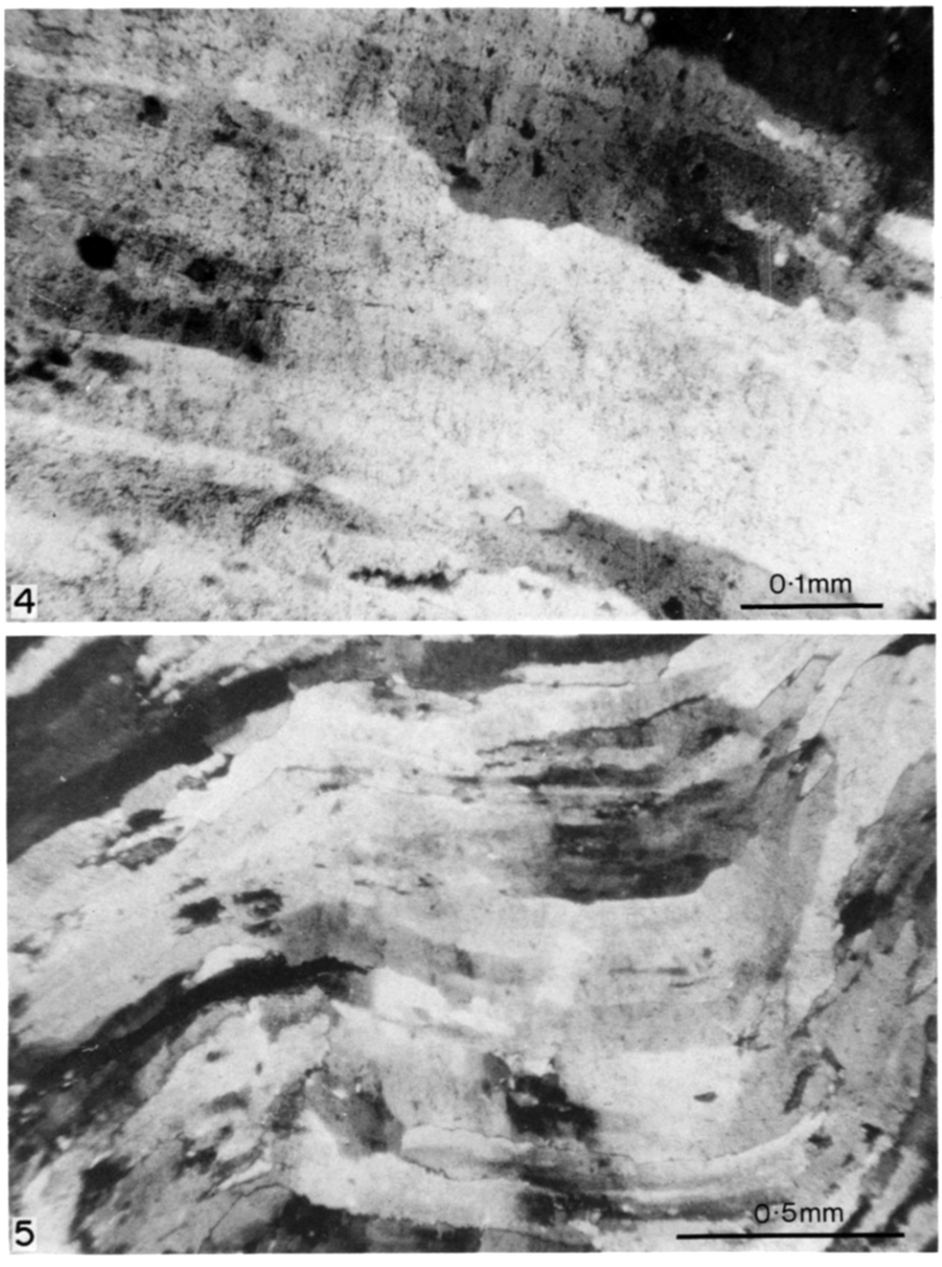

Fig. 4. Photomicrograph of quartz fibres in the extension veins. See text for discussion.

Fig. 5. Photomicrograph of deformation features in the extension veins. See text for discussion.

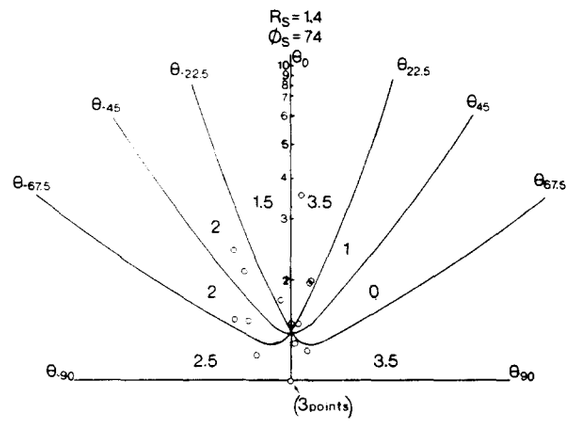

EXPECTED	E	2	2	2	2	2	2	2	2
OBSERVED	O	2.5	2	2	1.5	3.5	1	0	3.5

Fig. 6. Rf/ϕ plot on the hyperbolic net for deformed pebbles in the wallrock, using the method of De Paor (1981; cf. Robin 1977). θ-curves divide the plot into eight class intervals which should be equally populated for a perfectly uniform initial distribution. Values in the table show little departure from uniformity.

determined by fitting to the data set a 50%-of-data curve (Dunnet & Siddans 1971) or θ-45 curve (Lisle 1977) and noting its point of intersection with the stretch direction. The axial ratio obtained was Rs = 1.4. Uniformity of orientation of the initial pebble distribution was tested by superposing θ-22.5 and θ-67.5 curves (Fig. 6) (see also Robin 1977). Visual inspection of the expected vs observed population table reveals a clear pattern of uniformity, though the total population was too low for χ^2-squared testing.

An attempt to measure the amount of deformation in the shear zones between the en échelon veins failed as a result of the problem of scale. While an Rf/ϕ diagram could be constructed for such a domain (Fig. 7), it was found that the fluctuation of pebble orientations was too low for consistency with the estimated Rs value (Cloos 1947, Ramsay 1967, p. 203). This may be due to local non-uniformity of the initial distribution or to pressure-solution truncation of highly fluctuate pebbles, but is

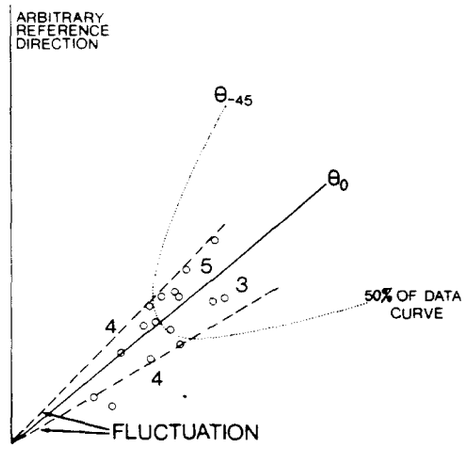

Fig. 7. Rf/ϕ plot on the hyperbolic net for deformed pebbles in a shear zone between the extension veins. Note the low fluctuation except for one point.

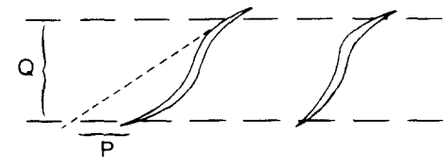

Fig. 8. Determination of shear strain from the zone-parallel deflection of an extension vein, P divided by the zone width, Q.

most likely due to heterogeneity of shear strain on the scale of the pebbles, fluctuate individuals being undersampled because of their non-elliptical shapes.

SHEAR ZONE DEFORMATION

We assumed that the state of deformation in each shear zone approximates to heterogeneous simple shear superimposed on homogeneous wallrock deformation, the increase in area caused by vein dilation being countered by pressure-solution cleavage formation. Small departures from this model do not cause large errors in the angular shears calculated. For example, a 10% shortening superimposed across a zone of 26.5° angular shear yields 29° angular shear, a change of only 10%.

We measured the angular shear, ψ, or shear strain, $\gamma = \tan(\psi)$ in each zone in two ways. First, we calculated the deflection of sigmoidal veins parallel to the zone, assuming that they were initially straight and that they propagated in a constant incremental direction (Fig. 8). If the deflection of a vein is P for a shear zone of width Q, then from the geometry shown in Fig. 8,

$$\gamma = P/Q. \quad (1)$$

Second, we noted the attitude of the cleavage trace (Fig. 9). In the absence of wall rock deformation, half γ

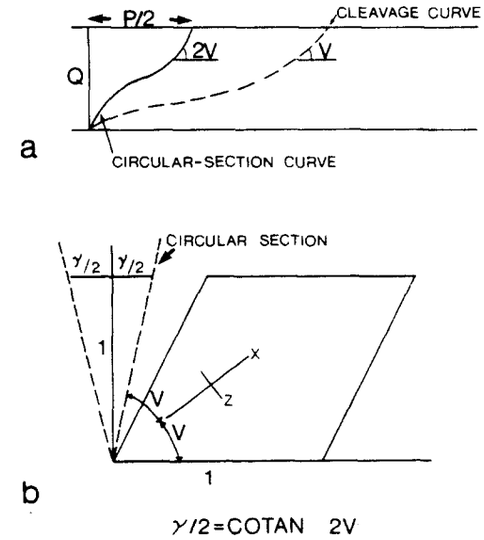

Fig. 9(a). Determination of shear strain from the cleavage trace assuming simple shear of undeformed wallrock. The circular section curve has twice the slope of the cleavage trace at every level in the zone. See text for explanation. (b) Theoretical justification for the method used in (a). X and Z are the left-principal stretches, V is the orientation of cleavage relative to the shear zone boundary and γ is the corresponding shear strain. See text for discussion.

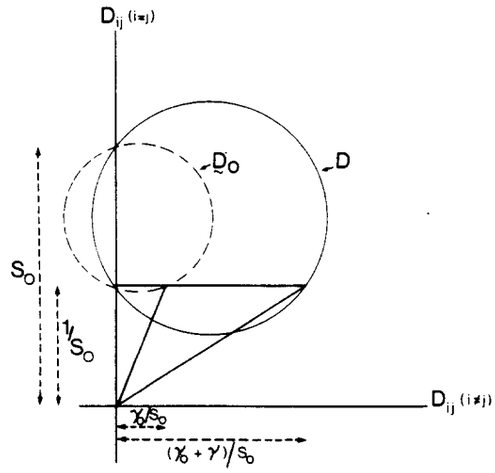

Fig. 10. Off-axis Mohr circle construction for the superposition of shear strain, γ, on a wallrock deformation represented by the dashed circle. The Mohr circle for the cumulative deformation (solid) must pass through $(0, S_0)$ and $((\gamma + \gamma_0)/S_0, 1/S_0)$. See text for discussion.

would be given by doubling the zone-parallel deflection of the cleavage curve and dividing by the thickness Q. The theoretical justification for this procedure is given in Fig. 9(b). Since the cleavage trace is assumed to lie in or near the XY plane of the left-stretch ellipsoid ($X > Y > Z$), it must bisect the angle between the circular sections. If V is the angle between the zone boundary and cleavage trace, then

$$\frac{\gamma}{2} = \text{Cot}\,(2V) \tag{2}$$

(Treagus 1981). Therefore, the cumulative deflection of the $2V$ curve across a zone of width Q is labelled $P/2$ in order that eqn. (1) again gives the cumulative shear strain.

Unfortunately, the cleavage trace in the shear zones records the total deformation which comprises homogeneous wall-rock deformation and superposed simple shear. This factorization is represented by the off-axis Mohr construction of Fig. 10 (see De Paor 1983, De Paor & Means 1984). Following Matthews *et al.* (1974), we represent the wall-rock deformation, $\mathbf{D}_0$, in upper triangular tensor form,

$$\mathbf{D}_0 = \begin{bmatrix} S_0 & S_0^{-1}\gamma_0 \\ 0 & S_0^{-1} \end{bmatrix}, \tag{3}$$

where S_0 is the zone parallel stretch and γ_0 the zone parallel shear strain required to change a unit circle into the shape of the left-stretch ellipse. Note that we may use the shape of the stretch ellipse to define the upper triangular tensor, $\mathbf{D}_0$, without making any assumption about the rotational or irrotational nature of the deformation (Matthews *et al.* 1974). The Mohr circle for this deformation is shown dashed in Fig. 10. It intersects the vertical axis in S_0 and $1/S_0$. Superposed simple shear has no effect upon the boundary direction of the shear zone. Therefore, the final Mohr circle (shown solid in Fig. 10) also passes through the S_0 and $1/S_0$ points, but a shear displacement of magnitude γ/S_0 must be applied to the level $1/S_0$ above the horizontal (zone parallel) axis. The final deformation state may be written

$$\mathbf{D} = \begin{bmatrix} S_0 & S_0^{-1}(\gamma_0 + \gamma) \\ 0 & S_0^{-1} \end{bmatrix}. \tag{4}$$

The required simple shear strain, γ, is thus the only non-zero element in the tensor $\mathbf{T}$,

$$\mathbf{T} = (\mathbf{D} - \mathbf{D}_0)S_0. \tag{5}$$

However, there is no obvious solution to eqn. (5) given only the wallrock stretch ratio of 1.4 and the internal and external cleavage traces. Therefore, we use a graphical solution based on the R/ϕ plot of Le Theoff (1979). Figure 11 is a logarithmic plot of axial ratio R vs orientation ϕ, measured positive clockwise from the pole to the shear zone. The arrowed lines on this plot represent the deformation paths followed by ellipses during dextral simple shear. The dashed lines are contours of shear strain with an interval of $\Delta\gamma = 0.2$. The point labelled (Ri, θ) is the wallrock deformation with θ measured

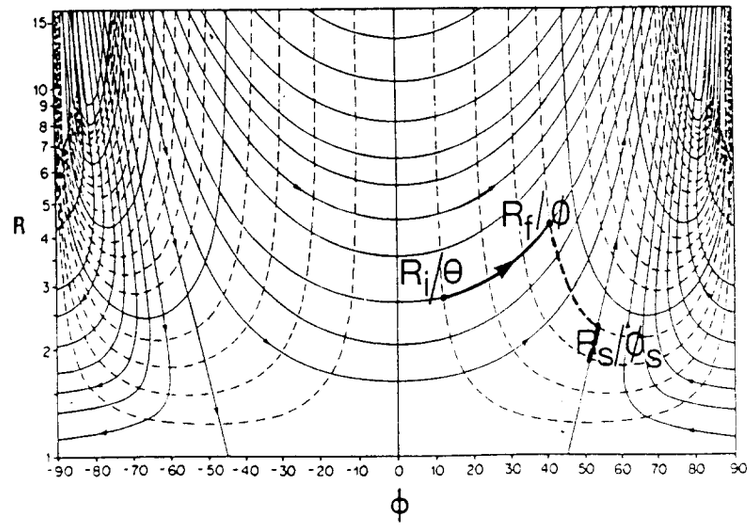

Fig. 11. Le Theoff's R/ϕ plot. (Ri, θ) represents the wallrock deformation. ϕs is the internal trace of cleavage. Rf is the internal left-stretch ratio. $(Rs, \phi s)$ represents the simple shear component of deformation. See text for discussion.

relative to a particular shear zone, and the direction labelled ϕ is the internal cleavage trace. To determine the component of simple shear in this case we simply follow the trajectory through (Ri, θ) till it intersects the ϕ direction at Rf and count the number of $\Delta\gamma$ contour intervals *en route*. To find the axial ratio Rs and orientation ϕs of the left-stretch ellipse corresponding to the measured shear strain γ, we simply set off $\Delta\gamma$ on the trajectory for an initial unit circle (which originates at [1, 45°]). The final point has coordinates (Rs, ϕs). The reader is reminded of the sign convention for angles plotted on the Le Theoff diagram: all angles are measured positive clockwise of the pole to the shear zone. Since this plot is symmetric about $\phi = 0$, it may be used to analyse sinistral shear zones simply by reversing the directions of the arrows on the trajectories.

By using two independent methods of shear strain determination, namely the zone-parallel deflection of sigmoidal veins and the Le Theoff plot as described above, we were able to detect breakdowns in our assumptions. Large differences in the shear strains determined by the two methods could be attributed to either non-simple shear or to brittle failure on discrete zone-parallel planes. Although the Ballyquin locality abounds in shear zones, our analysis was confined to a small area where problems such as brittle deformation did not appear to be significant.

BULK DEFORMATION

The veins of Ballyquin form an unusually regular lattice of parallel arrays (Fig. 2). Therefore, it was possible to carry out two traverses, one of which intersected only dextral zones, the other only sinistral zones. It was assumed that there was no rotation of the blocks of wall rock between the zones. The traverses were terminated by faults after four to six arrays had been sampled. Because the traverses were not mutually perpendicular it was necessary to use a general tensor method to obtain the bulk deformation state. First, the overall shear strain on each traverse was calculated as illustrated in Fig. 12. Then the reciprocal deformation tensor was constructed relative to the line of traverse as abscissa and its normal as ordinate,

$$\mathbf{D}_1^{-1} = \begin{bmatrix} 1 & 0 \\ -\gamma_1 & 1 \end{bmatrix} \tag{6}$$

where γ_1 is the bulk shear strain for the first traverse.

Then, the bulk reciprocal deformation tensor $\mathbf{D}^{-1}$ was calculated in the east-north reference frame,

$$\mathbf{D}^{-1} = \mathbf{R}_3\mathbf{D}_2^{-1}\mathbf{R}_2\mathbf{D}_1^{-1}\mathbf{R}_1 \tag{7}$$

where the tensors $\mathbf{R}$ are of orthonormal form,

$$\mathbf{R} = \begin{bmatrix} \text{Cos } \omega & -\text{Sin } \omega \\ \text{Sin } \omega & \text{Cos } \omega \end{bmatrix}, \tag{8}$$

representing a rigid rotation through an angle ω. $\mathbf{R}_1$ functions to rotate the first traverse into alignment with the arbitrary reference frame. $\mathbf{D}_1^{-1}$ represents the bulk

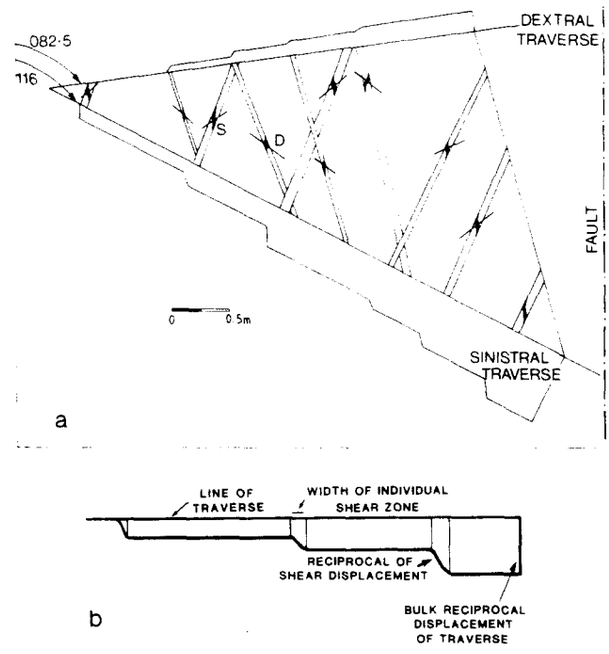

Fig. 12(a). Schematic plan view of the outcrop and (b) traverse across the shear zones.

reciprocal deformation of that traverse. $\mathbf{R}_2$ rotates the second traverse into alignment with the arbitrary reference frame. $\mathbf{D}_2^{-1}$ applies the bulk reciprocal deformation on that traverse. Finally, $\mathbf{R}_3$ restores the initial reference frame. In the present example, the tensor products of eqn. (7) had the following limiting values,

$$\omega_3 = 7\tfrac{1}{2}^\circ;\ -\gamma_2 = -0.3;\ \omega_2 = -33\tfrac{1}{2}^\circ;\ -\gamma_1 = 0.7;\ \omega_1 = 26^\circ \tag{9}$$

or

$$\omega_3 = -26^\circ;\ -\gamma_2 = 0.7;\ \omega_2 = 33\tfrac{1}{2}^\circ;\ -\gamma_1 = -0.3;\ \omega_1 = -7\tfrac{1}{2}^\circ \tag{10}$$

depending on the interpreted order of events, namely all dextral movement before sinistral (eqn. 9) and all sinistral before dextral (eqn. 10). Field observations suggest a natural deformation path intermediate between these extremes. By inversion of $\mathbf{D}^{-1}$ in eqn. (7), these values yield

$$\mathbf{D} = \begin{bmatrix} 1.26 & -0.04 \\ -0.34 & 0.8 \end{bmatrix} \text{ or } \mathbf{D} = \begin{bmatrix} 1.22 & -0.05 \\ -0.55 & 0.84 \end{bmatrix}. \tag{11}$$

The tensors $\mathbf{D}$ are represented by parallelograms in Fig. 13. They differ by little and clearly indicate an asymmetrical deformation with a right-lateral sense of rotation. The rotational component of 8–14° was obtained from the 'off-axis' Mohr construction. One side of the parallelogram is rotated through 90° and is then joined to the other. The Mohr circle is constructed on that join as diameter. The central axis of the Mohr circle is displaced from the reference axis by an angle equal in magnitude and sense to the rotational component of the deformation; in this case 8 or 14° depending on the inferred

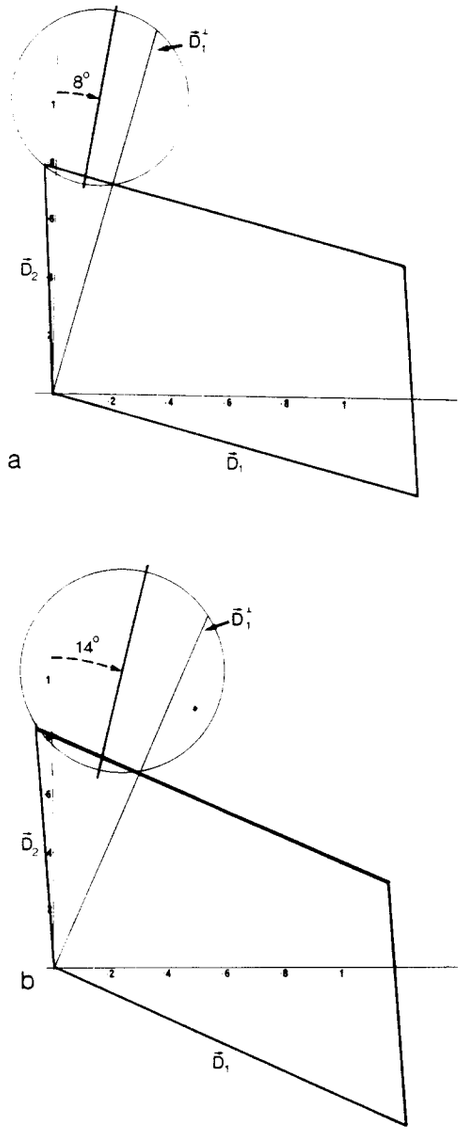

Fig. 13(a) and (b). Two interpretations of the deformed state represented by parallelograms. The off-axis Mohr circle indicates the rotational component of the deformation, ω. See text for explanation.

deformation path. Note also that the bulk stretch ratio of the outcrop which is due to vein formation alone is

$$R_s = 1.8 \quad (12)$$

if all dextral strain preceded sinistral, or

$$R_s = 2.01 \quad (13)$$

if all sinistral preceded dextral. Again, the true value is intermediate between these extremes since sinistral and dextral movements were penecontemporaneous.

DISCUSSION

We conclude that the Ballyquin outcrop has suffered significant overall shape change as a result of movements on individual shear zones and that the shape change was accompanied by an 8–14° clockwise rotation of the overall domain. The state of deformation is one of sub-simple shear in the terminology of De Paor (1983) because the rotational component is less than that appropriate to simple shear for the calculated amount of stretch.

We do not infer any overall sense of movement for the Hercynian Belt of Southern Ireland for the following reasons: (1) The above analysis is dependent on the validity of the assumptions that the shear zones were oriented symmetrically to bedding, that they developed by simple shear and that the internal X-direction lies close to the trace of cleavage. (2) The deformation measured was confined to a period of vein formation—only the stretch component of the homogeneous wall-rock deformation could be measured by the Rf/ϕ method; there may have been an associated rotational component which could not be detected by strain analysis. (3) The present study refers only to outcrop scale; regional patterns may differ from such local patterns.

Bearing these reservations in mind, our results, would appear to preclude any large component of strike slip in the strain history after vein development. Indeed, had the deformation of Southern Ireland been developed largely by wrench tectonics we would not expect conjugate sets of vein arrays to have developed. Low values of rotational strain imply a dominance of northerly compression over dextral wrenching, at least in this locality (see Cooper *et al.* in press). Our observations are consistent with the recent conclusions of Hancock *et al.* (1983) and Coward & Smallwood (1984). Nevertheless it has been demonstrated that rotational deformation can be detected given the correct combination of strain markers and that deformation confined to discrete shear zones can have a significant overall effect.

A final precautionary note: when we first carried out this analysis we used the theory outlined in Figs. 8 and 9, ignoring the state of deformation in the wall rock which appeared to be of little consequence, and concluded that the rotational component of bulk deformation was sinistral. Because the wall rock and shear zone stretch ratios are of the same order of magnitude, factorization using the Le Theoff plot is critical.

Acknowledgements—Denis Collins was financed by the Geological Survey of Ireland. Declan De Paor acknowledges grant support from the Atlantic Richfield Foundation, Conoco, Texaco and NSF Grant No. EAR 8211817. Dave Sanderson's critical review of an earlier draft drastically altered the appearance of the final version.

REFERENCES

Beach, A. 1975. The geometry of en-échelon vein arrays. *Tectonophysics* **28**, 245–263.

Cloos, E. 1947. Oolite deformation in the South Mountain Fold, Maryland. *Bull. geol. Soc. Am.* **58**, 843–918.

Collins, D. A. 1985. The structure and stratigraphy of the Clashmore–Helvick Head area of S.W. County Waterford. Unpublished Ph.D thesis, National University of Ireland.

Cooper, M. A., Collins, D., Ford, M., Murphy, F. X. & Trayner, P. M. 1984. Structural style, shortening estimates and the thrust front of the Irish Variscides. In: *Variscan Tectonics in the North Atlantic Region* (edited by Hutton, D. H. W. & Sanderson, D. J.). *Spec. Publs geol. Soc. London.* **14**, 167–175.

Cooper, M. A., Collins, D., Ford, M., Murphy, F. X., Trayner, P. M. & O'Sullivan, M. In press. Structural evolution of the Irish Variscides. *Spec. Publs geol. Soc. Lond.*

Coward, M. P. & Smallwood, S. 1984. An interpretation of the Variscan Tectonics of S.W. Britain. In: *Variscan Tectonics in the North Atlantic Region* (edited by Hutton, D. H. W. & Sanderson, D. J.). *Spec. Publs geol. Soc. Lond.* **14**, 89–102.

Dawson-Grove, G. E. 1955. Analysis of minor structures near Ardmore, County Waterford. *Q. Jl geol. Soc. Lond.* **111**, 1–21.

De Paor, D. G. 1981. Geological strain analysis. Unpublished Ph.D thesis, National University of Ireland, 104.

De Paor, D. G. 1983. Orthographic analysis of geological structures—I. Deformation theory. *J. Struct. Geol.* **5**, 255–277.

Dunnet, D. 1969. A technique of finite strain analysis using elliptical particles. *Tectonophysics* **7**, 117–136.

Dunnet, D. & Siddans, A. W. B. 1971. Non-random sedimentary fabrics and their modification by strain. *Tectonophysics* **12**, 307–325.

Hancock, P. L. 1972. The analysis of en echelon veins. *Geol. Mag.* **109**, 269–276.

Hancock, P. L., Dunne, W. M. & Tringham, M. E. 1983. Variscan deformation in southwest Wales. In: *The Variscan Fold Belt in the British Isles* (edited by Hancock, P. L.). Adam Hilger, Bristol, 47–73.

Hossack, J. R. 1979. The use of balanced cross sections in the calculation of orogenic contraction: a review. *J. geol. Soc. Lond.* **136**, 705–711.

Knipe, R. J. & White, S. H. 1979. Deformation in low grade shear zones in the Old Red Sandstone, S.W. Wales. *J. Struct. Geol.* **1**, 53–66.

Lajtai, E. Z. 1969. Mechanics of second order faults and tension gashes. *Bull. geol. Soc. Am.* **80**, 2253–2272.

Le Theoff, B. 1979. Non-coaxial deformation of elliptical particles. *Tectonophysics* **53**, T7–T13.

Lisle, R. J. 1977. Clastic grain shape and orientation in relation to cleavage from the Aberystwyth Grits, Wales. *Tectonophysics* **39**, 381–395.

Matthews, P. E., Bond, R. A. B. & Van Der Berg, J. J. 1974. An algebraic method of strain analysis using elliptical markers. *Tectonophysics* **24**, 31–67.

Ramsay, J. G. 1967. *Folding and Fracturing of Rocks*. McGraw-Hill, New York.

Ramsay, J. G. 1980. Shear zone geometry—a review. *J. Struct. Geol.* **2**, 83–99.

Ramsay, J. G. & Graham, P. H. 1970. Strain variation in shear belts. *Can. J. Earth Sci.* **7**, 787–813.

Ramsay, J. G. & Huber, M. 1983. *The Techniques of Modern Structural Geology. Vol. 1, Strain Analysis*. Academic Press, New York.

Robin, P. Y.-F. 1977. Determination of geological strain using randomly oriented strain markers of any shape. *Tectonophysics* **42**, T7–T16.

Roering, C. 1968. The geometric significance of natural crack arrays. *Tectonophysics* **5**, 107–123.

Treagus, S. H. 1981. A simple-shear construction from Thompson & Tait (1867). *J. Struct. Geol.* **3**, 291–293.